

Reproductive genetics

Circulating anti-Müllerian hormone levels in pre-menopausal women: novel genetic insights from a genome-wide association meta-analysis

Natàlia Pujol-Gualdo ^{1,2,†,*}, Minna K. Karjalainen ^{3,4}, Urmo Vösa ¹, Riikka K. Arffman ^{1,2}, Reedik Mägi ¹, Justiina Ronkainen ³, Triin Laisk ^{1,‡}, and Terhi T. Piltonen ^{1,2,‡}

¹Estonian Genome Centre, Institute of Genomics, University of Tartu, Tartu, Estonia

²Department of Obstetrics and Gynecology, Research Unit of Clinical Medicine, University of Oulu, Oulu, Finland

³Research Unit of Population Health, Faculty of Medicine, University of Oulu, Oulu, Finland

⁴Northern Finland Birth Cohorts, Arctic Biobank, Infrastructure for Population Studies, Faculty of Medicine, University of Oulu, Oulu, Finland

*Correspondence address. Department of Obstetrics and Gynecology, Research Unit of Clinical Medicine, University of Oulu, Oulu, Finland; Estonian Genome Centre, Institute of Genomics, University of Tartu, Tartu, Estonia. E-mail: npujolgualdo@gmail.com <https://orcid.org/0000-0001-6428-8427>

†This author is the first author.

‡These authors shared co-last authorship.

ABSTRACT

STUDY QUESTION: Can a genome-wide association study (GWAS) meta-analysis, including a large sample of young premenopausal women from a founder population from Northern Finland, identify novel genetic variants for circulating anti-Müllerian hormone (AMH) levels and provide insights into single-nucleotide polymorphism enrichment in different biological pathways and tissues involved in AMH regulation?

SUMMARY ANSWER: The meta-analysis identified a total of six loci associated with AMH levels at $P < 5 \times 10^{-8}$, three of which were novel in or near *CHEK2*, *BMP4*, and *EIF4EBP1*, as well as highlighted significant enrichment in renal system vasculature morphogenesis, and the pituitary gland as the top associated tissue in tissue enrichment analysis.

WHAT IS KNOWN ALREADY: AMH is expressed by preantral and small antral stage ovarian follicles in women, and variation in age-specific circulating AMH levels has been associated with several health conditions. However, the biological mechanisms underlying the association between health conditions and AMH levels are not yet fully understood. Previous GWAS have identified loci associated with AMH levels in pre-menopausal women, in or near *MCM8*, *AMH*, *TEX41*, and *CDCA7*.

STUDY DESIGN, SIZE, DURATION: We performed a GWAS meta-analysis for circulating AMH level measurements in 9668 premenopausal women.

PARTICIPANTS/MATERIALS, SETTING, METHODS: We performed a GWAS meta-analysis in which we combined 2619 AMH measurements (at age 31 years) from a prospective founder population cohort (Northern Finland Birth Cohort 1966, NFBC1966) with a previous GWAS meta-analysis that included 7049 pre-menopausal women (age range 15–48 years) (N = 9668). NFBC1966 AMH measurements were quantified using an automated assay. We annotated the genetic variants, combined different data layers to prioritize potential candidate genes, described significant pathways and tissues enriched by the GWAS signals, identified plausible regulatory roles using colocalization analysis, and leveraged publicly available summary statistics to assess genetic and phenotypic correlations with multiple traits.

MAIN RESULTS AND THE ROLE OF CHANCE: Three novel genome-wide significant loci were identified. One of these is in complete linkage disequilibrium with c.1100delC in *CHEK2*, which is found to be 4-fold enriched in the Finnish population compared to other European populations. We propose a plausible regulatory effect of some of the GWAS variants linked to AMH, as they colocalize with GWAS signals associated with gene expression levels of *BMP4*, *TEX41*, and *EIF4EBP1*. Gene set analysis highlighted significant enrichment in renal system vasculature morphogenesis, and tissue enrichment analysis ranked the pituitary gland as the top association.

LARGE SCALE DATA: The GWAS meta-analysis summary statistics are available for download from the GWAS Catalogue with accession number GCST90428625.

LIMITATIONS, REASONS FOR CAUTION: This study only included women of European ancestry and the lack of sufficiently sized relevant tissue data in gene expression datasets hinders the assessment of potential regulatory effects in reproductive tissues.

WIDER IMPLICATIONS OF THE FINDINGS: Our results highlight the increased power of founder populations and larger sample sizes to boost the discovery of novel trait-associated variants underlying variation in AMH levels, which aided the characterization of GWAS signals enrichment in different biological pathways and plausible genetic regulatory effects linked with AMH level variation for the first time.

Received: September 5, 2023. Revised: May 13, 2024. Editorial decision: May 16, 2024.

© The Author(s) 2024. Published by Oxford University Press on behalf of European Society of Human Reproduction and Embryology.

This is an Open Access article distributed under the terms of the Creative Commons Attribution-NonCommercial License (<https://creativecommons.org/licenses/by-nc/4.0/>), which permits non-commercial re-use, distribution, and reproduction in any medium, provided the original work is properly cited. For commercial re-use, please contact journals.permissions@oup.com

STUDY FUNDING/COMPETING INTEREST(S): This work has received funding from the European Union's Horizon 2020 Research and Innovation Programme under the MATER Marie Skłodowska-Curie Grant Agreement No. 813707 and Oulu University Scholarship Foundation and Paulon Säätiö Foundation. (N.P.-G.), Academy of Finland, Sigrid Jusélius Foundation, Novo Nordisk, University of Oulu, Roche Diagnostics (T.T.P.). This work was supported by the Estonian Research Council Grant 1911 (R.M.). J.R. was supported by the European Union's Horizon 2020 Research and Innovation Program under Grant Agreements No. 874739 (LongITools), 824989 (EUCAN-Connect), 848158 (EarlyCause), and 733206 (LifeCycle). U.V. was supported by the Estonian Research Council grant PRG (PRG1291). The NFBC1966 received financial support from University of Oulu Grant No. 24000692, Oulu University Hospital Grant No. 24301140, and ERDF European Regional Development Fund Grant No. 539/2010 A31592. T.T.P. has received grants from Roche, Perkin Elmer, and honoraria for scientific presentations from Gedeon Richter, Exeltis, Astellas, Roche, Stragen, Astra Zeneca, Merck, MSD, Ferring, Duodecim, and Ajaton Terveys. For all other authors, there are no competing interests.

Keywords: anti-Müllerian hormone / genome-wide association study / low-frequency variants / reproductive ageing / reproductive genetics

Introduction

Anti-Müllerian hormone (AMH) is a member of the transforming growth factor β (TGF- β) superfamily, which includes the bone morphogenic proteins (BMPs), growth differentiation factors, activins, and inhibins. Despite owing its name to its classical role in male sexual differentiation, AMH is also expressed by the ovarian granulosa cells during the primary to small antral stage of follicle development (Weenen et al., 2004). In adult women, serum AMH levels decrease with age, with undetectable levels following menopause, signalling depletion of ovarian reserve (Finkelstein et al., 2020). As a result, AMH is primarily known as a serum marker for ovarian reserve. Previous studies have indicated that variations in age-specific circulating AMH levels are linked with several health conditions, including breast cancer (Ge et al., 2018) and PCOS (Homburg and Crawford, 2014). Therefore, identifying genetic determinants of inter-individual variation in AMH measurements may offer valuable insight into their biological mechanistic effects and impact on health and disease beyond reproductive ageing.

Three previous genome-wide association studies (GWAS) have identified a few loci associated with AMH levels in pre-menopausal women (Schuh-Huerta et al., 2012; Ruth et al., 2019; Verdiesen et al., 2022). These studies have had progressively increasing sample sizes ($n = 232\text{--}7049$) and lately have also started to incorporate a group of younger women in the meta-analysis (Verdiesen et al., 2022). However, larger sample sizes are key to unravelling potential new loci with variation in AMH levels. While AMH levels typically decrease with age, the inclusion of a younger cohort to the study adds an extra value to the meta-analysis. Since younger women will likely exhibit more variation in AMH measurements, this wider variation of AMH values enhances the power of genome-wide association analysis in detecting significant genetic variations that are linked to a wider distribution of values. The current work analyses data from a single time point measured in relatively young pre-menopausal women and combines this dataset with a previous meta-analysis (Verdiesen et al., 2022), to identify and characterize additional loci associated with AMH levels in pre-menopausal women.

The studies conducted so far have focused on European ancestry, mainly powered to discover associations with common genetic variants. Nonetheless, founder populations such as those found in northern Finland, represent a powerful resource to accelerate discovery of new biological mechanisms driven by low-frequency alleles that have risen to higher frequency owing to the unique demographic history (Kurki et al., 2023).

In the present study, we added 2619 AMH measurements (at age 31 years) from a prospective founder population cohort (Northern Finland Birth Cohort 1966, NFBC1966) to a previous GWAS meta-analysis of 7049 pre-menopausal women (age range

15–48 years) (Verdiesen et al., 2022), reaching the largest sample size for assessing AMH variation in women from reproductive age to date ($N = 9668$). Beyond detecting three out of the four previously identified signals near testis expressed 41 (TEX41), mini-chromosome maintenance 8 homologous recombination repair factor (MCM8) and AMH, we identified three novel signals near eukaryotic translation initiation factor 4E binding protein 1 (EIF4EBP1), bone morphogenic protein 4 (BMP4), and checkpoint kinase 2 (CHEK2). In the CHEK2 locus, the c.1100delC variant is enriched in the Finnish population and in complete linkage disequilibrium (LD) ($r^2 = 1$) with the lead variant identified in that locus. Additionally, we tested regulatory effects of GWAS variants on specific genes and gene transcript expression in multiple tissues using colocalization analysis, evaluated gene set and tissue set enrichments, and estimated genetic correlations and phenotypic associations across multiple phenotypes, by leveraging publicly available summary statistics.

Materials and methods

Study design and setting

This study is based on the prospective population-based NFBC1966 study (University of Oulu, 1966, <http://urn.fi/urn:nbn:fi:att:bc1e5408-980e-4a62-b899-43bec3755243>). During 1966, 12 231 children (5889 females) were born in the two northernmost provinces of Finland (covering 48% of Finnish territory). Originally, the study was set to evaluate the impact of early life factors on long-term health and work ability. The cohort population has been followed up at four different time points: 1, 14, 31, and 46 years of age (set by the cohort centre). Comprehensive questionnaires on female health and clinical examinations with biological data collection were performed at ages 31 and 46 years.

The detailed cohort description and follow-up protocol have been previously published (Nordström et al., 2022). Briefly, in 1997 (the 31-year follow-up) women living in the Northern Finland area or in the Helsinki metropolitan area ($n = 4074$ women) were invited to a clinical examination, in which 3127 (77%) women participated. The present study includes 2619 women with AMH and genetic data available at 31 years old (median = 31.1, interquartile range (IQR) = 30.9–31.4).

For the meta-analysis, publicly available summary statistics from an independent second study evaluating AMH variations across 7049 pre-menopausal women were used (Verdiesen et al., 2022). Publicly available summary statistics were downloaded from the GWAS catalogue (<https://www.ebi.ac.uk/gwas/publications/35274129>) under accession number GCST90104596. This study included data from the AMH GWAS meta-analysis by Ruth et al. (2019) ($n = 3334$), which meta-analysed four studies, and three cohorts which were additionally analysed and joined to the latter, resulting in the most recent meta-analysis ($n = 7049$)

(Verdiesen et al., 2022). The cohort details from the current meta-analysis ($n=9668$) can be found in [Supplementary Table S1](#). More details of the cohort description of the studies included can be found in (Verdiesen et al., 2022). All studies had received ethical approval from institutional ethics committees.

AMH measurement in NFBC1966

Serum samples were drawn in 1997 (the 31-year follow-up), sealed, and have been stored at -20°C since then. Serum AMH concentrations were measured using the automated Elecsys[®] electrochemiluminescence immunoassay on a Cobas E411 analyser according to the manufacturer's instructions (Roche Diagnostics, Mannheim, Germany). More detailed information on AMH measurement has been published previously (Piltonen et al., 2023).

The assay limits of detection and quantitation were, respectively, 0.01 ng/ml and 0.03 ng/ml for AMH. Intra- and inter-assay coefficients of variance were 1.0–1.8% and 2.9–4.4% for AMH, respectively. Limits above the measuring ranges were 23 ng/ml for AMH.

AMH concentrations were converted to pmol/l using $1\text{ ng/ml} = 7.14\text{ pmol/l}$. As AMH levels are not normally distributed, for the following analysis AMH measurements were transformed using rank-based inverse normal transformation, as carried out previously (Ruth et al., 2019). For rank-based inverse normal transformation, we used the package *RNOmni* in R v3.6.3. (McCaw et al., 2020).

Genotyping details and association analysis

Genotyping of the NFBC1966 samples was performed with the Illumina Infinium HumanCNV370-Duo array (Illumina, San Diego, CA, USA). Samples were excluded based on call rate $<95\%$, gender mismatch, relatedness (identity by descent estimate $\text{pihat} > 0.2$), and outlying heterozygosity. Single-nucleotide polymorphisms (SNPs) were excluded based on missingness rate $>5\%$, Hardy–Weinberg equilibrium $P < 0.000001$, and minor allele frequency (MAF) $<1\%$. Genotypes were imputed with Beagle 4.1 using the SiSu v3 imputation reference panel, which consisted of 3775 individuals of Finnish ancestry with sequenced whole genomes.

Association analysis was performed using SNPTEST v2.5.4-beta1, adjusted by the first 10 genetic principal components. Markers with INFO score >0.4 were kept for the meta-analysis. Positions were converted to build hg37 to harmonize the data with the summary statistics available from Verdiesen et al. before running the meta-analysis, using LiftOver (Kent et al., 2002).

GWAS meta-analysis

We conducted an inverse variance weighted fixed-effects meta-analysis with single genomic control correction using GWAMA software (v2.2.2) (Mägi and Morris, 2010). A total of 13 903 812 variants were included in the meta-analysis of 9688 AMH measurements. After meta-analysis, we kept variants present in both studies (totalling 7 900 839 variants) for downstream analysis. Using GWAMA (v2.2.2), we ran two tests of heterogeneity (Q-Cochran test and heterogeneity index (I^2) of effects across the studies meta-analysed). Lead SNPs were identified as single nucleotide variants independent from each other with $P\text{-value} \leq 5 \times 10^{-8}$. The maximum distance between LD blocks of independent SNPs to merge into a single genomic locus was set to 500 kb. Regional plots of each locus are presented in [Supplementary Fig. S1](#).

Heritability analysis

The heritability (h^2) was estimated by single-trait LD score regression using the meta-analysis summary statistics and HapMap 3 LD-scores using LDSC v1.0.1 (<https://github.com/bulik/ldsc>) (Bulik-Sullivan et al., 2015).

Annotation of GWAS signals

We used FUMA (v1.4.0) to annotate the GWAS signals (Watanabe et al., 2017). FUMA is an online platform that performs annotation of GWAS signals using data from several databases. First, FUMA identifies lead SNPs ($P\text{-value} \leq 5 \times 10^{-8}$ and SNP pairwise LD $r^2 < 0.1$, based on 1000G European reference) and independent significant SNPs and each risk locus ($P\text{-value} < 5 \times 10^{-8}$ and LD $r^2 < 0.6$) ([Supplementary Tables S2 and S3](#)). Then FUMA identifies potential candidate SNPs that are in LD with any of the identified independent significant SNPs and annotates them via linking with several databases (ANNOVAR, RegulomeDB, CADD scores, etc.), which gives information on their location, functional impact, and potential regulatory effects.

Colocalization analysis

We used HyPrColoc (Foley et al., 2021), a colocalization method for identifying the overlap between our GWAS meta-analysis signals and cis-quantitative trait loci (cis-QTL) signals from different tissues and cell types (expression QTLs, transcript QTLs, exon QTLs, and exon usage QTLs available in the eQTL Catalogue; Kerimov et al., 2021). We lifted the GWAS summary statistics over to hg38 build to match the eQTL Catalogue using binary liftOver tool (https://genome.sph.umich.edu/wiki/LiftOver#Binary_liftOver_tool).

For the genome-wide significant ($P \leq 5 \times 10^{-8}$) GWAS loci identified we extracted the ± 500 kb of its top hit from QTL datasets and ran the colocalization analysis against eQTL Catalogue traits. For each eQTL Catalogue dataset, we included all the QTL features which shared at least 80% of tested variants with the variants present in our GWAS region. We used the default settings for HyPrColoc analyses and did not specify any sample overlap argument, because HyPrColoc paper (Foley et al., 2021) demonstrates that assuming trait independence gives reasonable results. HyPrColoc outputs the posterior probability that genetic association signals for those traits are colocalizing (we considered two or more signals to colocalize if the posterior probability for a shared causal variant (PP4) was 0.8 or higher). All results with a PP4 > 0.8 can be found in [Supplementary Table S4](#).

Gene prioritization

In order to nominate plausible candidate genes in each locus, we prioritized genes according to different levels of evidence: genes containing lead variants that are coding variants or coding variants in high LD ($r^2 > 0.6$) with lead variants; genes whose expression was regulated by eQTL variants that showed significant (posterior probability > 0.8) colocalization with our GWAS signals; and genes which showed a plausible biological role as defined previously in the research literature.

Gene set and tissue set enrichment analyses

Gene set enrichment analysis and tissue set enrichment analysis were performed using MAGMA v1.08 implemented in FUMA v1.4.0. Gene sets were obtained from Msigcbv7.0 for 'Curated gene sets' and gene ontology ('GO' terms). A total of 15 485 gene terms were queried. The results of this analysis are presented in [Supplementary Table S5](#) and [Fig. S2](#). Tissue expression analysis was performed for 53 tissue types using MAGMA. The results of

this analysis are presented in [Supplementary Table S6](#) and [Fig. S2](#).

Genetic correlation analysis

The Complex Traits Genetics Virtual Lab (CTG-VL, <https://vl.genoma.io/>) was used to calculate genetic correlations between the AMH meta-analysis and 1335 traits. We applied a multiple testing correction (Benjamini–Hochberg false discovery rate (FDR) <5%) to determine statistical significance using the *p.adjust* function in R 3.6.3. Results of the genetic correlation analysis are presented in [Supplementary Fig. S3](#) and [Table S7](#).

Phenome-wide associations

We evaluated the association of our GWAS lead variants and variants in high LD with these by using human health traits and phenotypes available in the GWAS Catalogue (e0_r2022-11-29) as implemented in FUMA. We also queried the lead variants of this study from the FinnGen study (data freeze 9, total $n = 377\,277$), which combines samples collected from Finnish biobanks to digital healthcare data ([Kurki et al., 2023](#)). The results obtained are found in [Supplementary Table S8](#) and [Fig. S4](#).

Results

GWAS for AMH levels

To detect genetic factors associated with circulating AMH levels, we performed a GWAS meta-analysis with data from two studies (NFBC1966 GWAS and summary statistics publicly available from [Verdiesen et al., 2022](#)), including a total of 9668 AMH measurements quantified from women of pre-menopausal age and European ancestry.

The meta-analysis identified a total of six associated loci, with six independent signals significantly associated with AMH levels ($P \leq 5 \times 10^{-8}$) ([Table 1](#), [Supplementary Fig. S1](#)). A total of 70 SNPs reached genome-wide significance ($P \leq 5 \times 10^{-8}$).

Three of the associated loci were previously reported and were located in or near AMH (rs10417628, $P = 9.34 \times 10^{-9}$), TEX41 (rs6729614, $P = 1.68 \times 10^{-10}$), and MCM8 (rs16991615, $P = 4.68 \times 10^{-9}$) ([Ruth et al., 2019](#); [Verdiesen et al., 2022](#)), and three of the associated loci were novel. The novel loci included associations near EIF4EBP1 (rs10093345, $P = 9.34 \times 10^{-9}$), BMP4 (rs762643, $P = 1.98 \times 10^{-9}$), and CHEK2 (rs186430430, $P = 9.69 \times 10^{-11}$) ([Fig. 1](#), [Table 1](#)). All lead variants were present in the two datasets

analysed, and the directions of effects were consistent between the datasets for all six lead variants ([Fig. 2](#)). According to I^2 heterogeneity index and Q-Cochran P-value, none of the lead signals indicated any heterogeneity between the studies (I^2 index being 0% for the six lead signals and Q-Cochran P ranging from 0.37 to 0.99, with a Bonferroni corrected threshold of $0.05/6 = 0.008$).

There was no evidence of excessive genomic inflation ($\lambda = 1.01$) in the GWAS meta-analysis (LD score regression (LDSC) intercept = 1.0039 (SE 0.0076)). The observed scale SNP heritability estimate was 0.13 (SE 0.05).

Characterization of GWAS signals

Two out of the six lead variants that were detected are non-synonymous, making them notably easier to interpret and establishing a more solid foundation for pinpointing potential candidate genes. These non-synonymous variants are found in AMH (rs10417628 in chromosome 19, $P = 9.56 \times 10^{-12}$) and MCM8 (minichromosome maintenance 8 homologous recombination repair factor) (rs16991615 in chromosome 20, $P = 4.68 \times 10^{-9}$) and were previously described to be associated with AMH levels ([Ruth et al., 2019](#); [Verdiesen et al., 2022](#)).

In the novel locus identified on chromosome 22, the lead variant is an intronic variant near CHEK2 (rs186430430, $P = 9.69 \times 10^{-11}$). Interestingly, this variant is in complete LD ($r^2 = 1$) with the frameshift variant c.1100delC in CHEK2 (rs555607708). Despite complete LD, this rare variant is only found in the association analysis of the NFBC1966 GWAS, showing a P-value of 6.69×10^{-05} and beta of 0.79 (SE = 0.12) in this cohort only and not found in the summary statistics results from [Verdiesen et al., \(2022\)](#) likely explained by the fact that this variant is enriched in the Finnish population (MAF = 0.008) compared to other European populations (MAF = 0.002), and thus better powered to be captured in a GWAS setting including the former population in the analysis.

For the other three loci identified on chromosomes 2, 8, and 14, we defined for the first time plausible shared causal variants between GWAS signals and transcript and gene expression in specific tissues by colocalization analysis. This resulted in the prioritization of three plausible candidate genes, respectively: TEX41, EIF4EBP1, and BMP4 ([Supplementary Table S3](#)).

For instance, the association signal in chromosome 2, in an intronic region of TEX41, colocalized with eQTL signals for TEX1 transcripts ENST00000414256 in the testis (PP4 = 0.99) and

Table 1. Genome-wide significant signals in the meta-analysis for inverse normally transformed anti-Müllerian hormone levels in women.

rsID (lead variant)	Chromosome	Position (based on build 37)	Effect allele	Effect frequency (EUR/FINN)	Beta (SE)	P-value	Candidate gene	Source of support for candidate gene prioritization
rs6729614	2	145644874	G	0.26/0.25	0.08 (0.01)	5.56×10^{-11}	ZEB2/TEX41	Colocalization analysis and biological plausibility
rs10093345	8	37872776	T	0.72/0.68	-0.08 (0.01)	5.05×10^{-09}	EIF4EBP1	Colocalization analysis and biological plausibility
rs762643	14	54422767	T	0.44/0.41	-0.07 (0.01)	3.99×10^{-09}	BMP4	Colocalization analysis and biological plausibility
rs10417628	19	2251817	C	0.97/0.99	0.32 (0.04)	9.56×10^{-12}	AMH	Coding variant and biological plausibility
rs16991615	20	5948227	A	0.06/0.02	0.16 (0.02)	4.68×10^{-9}	MCM8	Coding variant and biological plausibility
rs186430430	22	29103598	C	0.002/0.008	0.79 (0.12)	9.69×10^{-11}	CHEK2	Frameshift variant c.1100delC in high LD with the lead variant

SNPs showing the most significant associations at each locus are shown, and novel genome-wide significant signals are highlighted in bold. Significance was set at $P \leq 5 \times 10^{-8}$.

EUR, European (non-Finnish); FINN, European (Finnish); SNP, single-nucleotide polymorphism; AMH, anti-Müllerian hormone; BMP4, bone morphogenetic protein 4; CHEK2, checkpoint kinase 2; EIF4EBP1, eukaryotic translation initiation factor 4E binding protein 1; MCM8, minichromosome maintenance 8 Homologous Recombination Repair Factor; TEX41, testis expressed 41.

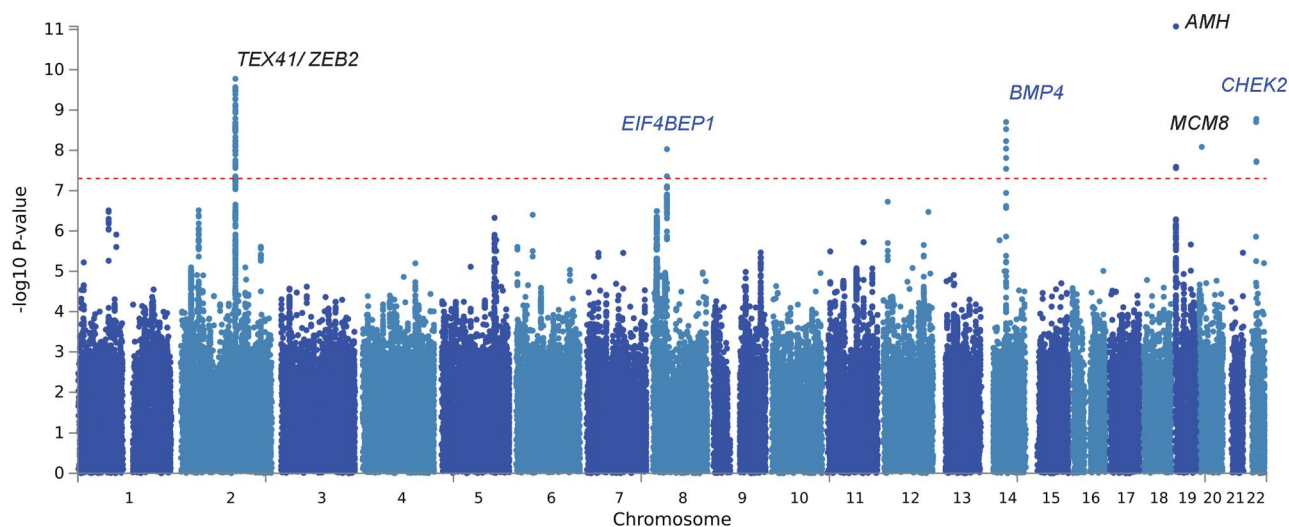


Figure 1. Manhattan plot for a genome-wide association study meta-analysis for anti-Müllerian hormone levels in pre-menopausal women ($n = 9668$). The novel loci are highlighted in blue. The y axis represents $-\log_{10}(P\text{-values})$ for association of variants with AMH levels and the x axis represents the chromosomal positions of the variants. The red horizontal dashed line represents the threshold for genome-wide significance ($P < 5 \times 10^{-8}$). AMH, anti-Müllerian hormone; BMP4, bone morphogenetic protein 4; CHEK2, checkpoint kinase 2; EIF4EBP1, eukaryotic translation initiation factor 4E binding protein 1; MCM8, minichromosome maintenance 8 homologous recombination repair factor; TEX41, testis expressed 41.

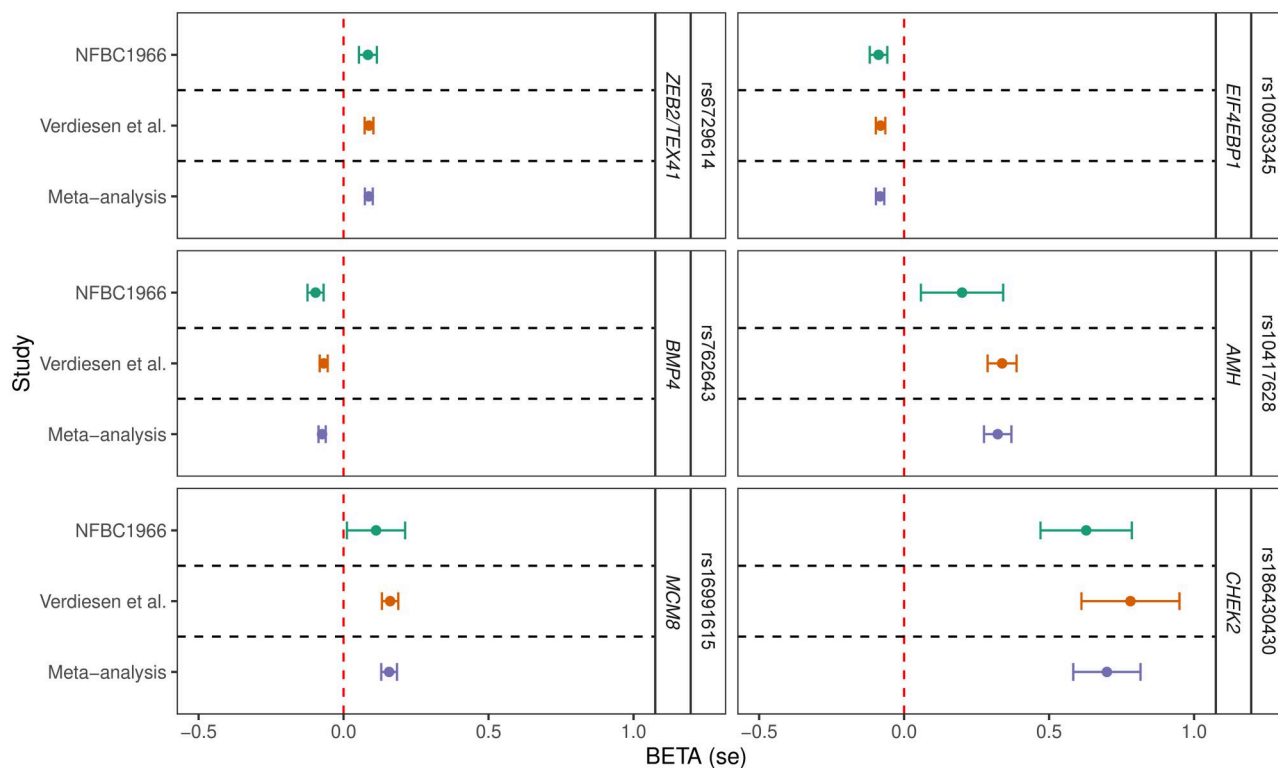


Figure 2. Forest plot of effect estimates for the six lead variants associated with anti-Müllerian hormone levels across datasets meta-analysed. The betas and standard errors are shown for the two studies meta-analysed (NFBC1966 (green dots, $n=2619$), Verdiesen et al. (2022) (orange dots, $n=7049$), and the presented largest meta-analysis (meta-analysis, purple dots, $n=9668$)). Candidate genes are also shown next to each genetic lead signal. Betas represent the effect sizes of each genetic variant association to phenotype, assessing the same risk allele across cohorts (effect allele and effect allele frequency are reported in Table 1). AMH, anti-Müllerian hormone; BMP4, bone morphogenetic protein 4; CHEK2, checkpoint kinase 2; EIF4EBP1, eukaryotic translation initiation factor 4E binding protein 1; MCM8, minichromosome maintenance 8 homologous recombination repair factor; TEX41, testis expressed 41.

ENST00000445791 in the skin ($PP4 = 1$). EIF4EBP1 was also prioritized based on colocalization evidence in three tissues, with high colocalization probability ($PP4 = 0.90$) between the GWAS signal

and cis-eQTLs for EIF4EBP1 expression in brain frontal cortex tissue, and between the GWAS signal and cis-eQTLs for EIF4EBP1 expression in left heart ventricle. Additionally, the GWAS

association signal in chromosome 8 showed colocalization with cis-eQTLs for BMP4 transcripts ENST00000245451 and ENST00000558489 in colon transverse (PP4 = 0.84) and BMP4 transcript ENST00000558489 in tibial nerve.

From colocalization results, only in the locus of chromosome 2, we observed that the associations might be explained by a single variant. Namely, we observed that the non-coding transcript (TEX41) exon variant rs17407477 and the intronic variant rs786244 were explaining most of the shared association, for the testis transcript expression association (posterior inclusion probability 0.90) and the skin transcript expression association (posterior inclusion probability 0.94), respectively.

Although we identified three out of the four signals that were previously reported in [Verdiesen et al., \(2022\)](#), we were unable to detect the signal near CDCA7 described in the past work (rs11683493 (T), $P = 1.7 \times 10^{-8}$). In our analysis using the NFBC66 GWAS data, this variant showed a P-value of 0.09 and therefore, the resulting P-value from the meta-analysis remained below the threshold of significance ($P = 1.02 \times 10^{-5}$). Although there might be various sources of variability which explain this discrepancy in our findings, we hypothesize the difference in sample size to be the primary reason.

Gene set and tissue set enrichment analyses

Gene set enrichment analysis highlighted significant enrichment of renal system vasculature morphogenesis ($P = 5.2 \times 10^{-8}$), glomerulus vasculature morphogenesis ($P = 1.77 \times 10^{-7}$), and glomerulus morphogenesis ($P = 2.99 \times 10^{-6}$) ([Supplementary Table S4](#) and [Fig. S2](#)). Tissue expression analysis yielded the strongest enrichment in the pituitary gland, even though not reaching significance after multiple testing correction ($P_{\text{non-adj}} = 0.02$) ([Supplementary Fig. S2](#) and [Table S6](#)).

Genetic correlations of AMH levels with diseases and traits

From genetic correlation analysis assessing the relation between AMH levels and 1335 traits (summary statistics for those traits are found at <http://www.nealelab.is/uk-biobank/>), three traits reflecting menopausal timing remained significant after FDR correction, all displaying very high genetic correlations with AMH levels: 'Age at menopause' ($r_g = 0.95$, $SE = 0.21$, $P = 8.85 \times 10^{-6}$), 'Had menopause' (referring to having already undergone menopause) ($r_g = -0.99$, $SE = 0.22$, $P = 1.56 \times 10^{-5}$), and 'Age started hormone-replacement therapy (HRT)' (age for initiation of HRT) ($r_g = 0.92$, $SE = 0.21$, $P = 2.05 \times 10^{-5}$). Additionally, we observed a range of nominally significant associations ($P < 0.05$) with traits spanning reproductive/hormonal traits (such as polyp of female genital tract and female genital prolapse), metabolic traits such as inverse relation with HbA1c, and positive correlations with neoplasms such as breast and bowel cancer ([Supplementary Fig. S3](#) and [Table S7](#)).

Phenome-wide association study

To get more insights into phenotypic manifestations of the AMH-associated variants, we performed a phenome-wide association study using the GWAS Catalogue. We detected that associated variants in the six loci identified had associations across several traits, ranging from cardiovascular traits, age at menopause, estradiol levels, heel bone mineral density, breast cancer, uterine fibroids, PCOS to blood cell counts ([Supplementary Table S7](#) and [Fig. S4](#)).

We performed a further look-up of the lead variants in the FinnGen study (data freeze 9, total $n = 377\,277$), which combines samples collected from Finnish biobanks with digital healthcare

data. We detected that two of the lead variants had associations ($P < 1 \times 10^{-5}$) with outcomes in FinnGen. rs762643 (near BMP4) associated with cervical disc disorders and hernia, while rs186430430 (near CHEK2) associated with a variety of outcomes including diseases of the genitourinary tract, different neoplasms (e.g. leiomyoma of uterus, neoplasms of ovary), and breast-cancer-related outcomes ([Supplementary Table S8](#)).

Discussion

Our GWAS meta-analysis of circulating AMH measurements in 9668 pre-menopausal women, including 2619 measurements from women at age 31 years from the NFBC1966, identified three novel association signals near EIF4EBP1, BMP4, and CHEK2. We also detected three previously identified signals near TEX41, MCM8, and AMH ([Verdiesen et al., 2022](#)).

CHEK2 was one of the most interesting associated loci. Of note, the lead variant near CHEK2 (rs186430430, $P = 9.69 \times 10^{-11}$, $MAF = 0.002$) is in complete LD ($r^2 = 1$) with a frameshift variant, c.1100delC (rs555607708, found in NFBC GWAS only, $P = 6.69 \times 10^{-05}$, odds ratio = 1.87, 95% CI = 1.37–2.55), as it is enriched in the Finnish population ($MAF = 0.008$) compared to other non-Finnish and non-Estonian European populations ($MAF = 0.002$) ([Tyrmä et al., 2022](#)). Apart from being known as a moderate risk gene for breast cancer, different GWAS highlighted loss of function alleles in CHEK2 to be associated with firstly, PCOS ([Tyrmä et al., 2022](#)) and secondly, with ovarian ageing (assessed as age at natural menopause) ([Ruth et al., 2021](#)). Furthermore, recent research on exome data has also identified an association between CHEK2 truncating variants (excluding c.1110delC) and later age at menarche ([Kentistou et al., 2023](#)).

CHEK2 encodes a checkpoint kinase 2, which induces cell cycle arrest and apoptosis in response to DNA damage ([Ahn et al., 2004](#)), also in oocytes with unrepaired DNA damage ([Ruth et al., 2021](#)). In the work from [Ruth et al., \(2021\)](#), Chek2^{-/-} female mice showed reduced follicular atresia around reproductive senescence, increased follicular response to gonadotrophin stimulation, and also elevated AMH levels around reproductive senescence. Our finding goes in line with this research and supports the hypothesis that loss of function in CHEK2 might result in decreased follicular atresia and higher AMH levels also in young premenopausal women.

In our general meta-analysis, we also detected previously identified associations of a missense variant in MCM8 ([Ruth et al., 2019](#); [Verdiesen et al., 2022](#)), a known DNA repair gene ([Park et al., 2013](#)). This missense variant has been associated previously with premature ovarian insufficiency (POI), infertility, age at menopause ([Day et al., 2015](#)), and cancer ([Michailidou et al., 2017](#); [Griffin and Trakselis, 2019](#); [Lutzmann et al., 2019](#)). However, this association was the weakest in NFBC66 alone. While this could support an age-specific effect of the missense variant, as supported in [Verdiesen et al. \(2022\)](#) upon identifying a negative effect direction for the cohort including adolescents versus older cohorts, this discrepancy might be as well due to the variant's lower frequency in the Finnish population ($MAF = 0.02$ compared to $MAF = 0.06$ in other European populations) and a smaller sample size in the NFBC1966 study. Further research including age-stratified groups with AMH levels available and genetic data might inform potential age-specific effects of genetic signals.

Regarding the missense variant in the AMH gene also reported in [Verdiesen et al. \(2022\)](#), the association between the missense variant rs10417628 in the AMH gene and AMH levels remains unclear in the current analysis. A case report from 2020

suggested that this variant reduces AMH detection without affecting its bioactivity (Hoyos et al., 2020). Previous GWAS meta-analysis (Verdiesen et al., 2022) also provided inconclusive results owing to inconsistent evidence from different assay data. In the NFBC66 study using an automated assay (Elecsys® AMH Plus, Roche Diagnostics, Mannheim, Germany), the missense variant showed a P-value of 0.15 ($n = 2619$), supporting the hypothesis of a detection issue rather than an actual difference in AMH bioactivity. However, comparing AMH values from different assays remains problematic, and recent evidence suggests lower values in automated assays compared to AMH GenII ELISA assay (Beckman Coulter UK Ltd, High Wycombe, UK) and picoAMH ELISA (Ansh Labs, Webster, TX, USA) (Moolhuijsen and Visser, 2020). Further research is needed to validate the association between rs10417628 and AMH levels using different cohorts which have availability of both individual-level data and measurements obtained from different assays.

Colocalization analysis supports regulatory effects of GWAS variants associated with AMH with genetic variants modifying expression levels of *TEX41*, *BMP4*, and *EIF4EBP1* and thus provides a refinement for the characterization of possible regulatory effects of the genetic variants on different transcripts and genes.

Interestingly, we observed high posterior probability ($PP4 = 0.99$) of colocalization between our GWAS signal and eQTL signal for the *TEX41* (Testis expressed 41) transcript ENST00000414256 in the testis, prioritizing this long non-coding RNA gene for the first time in association with AMH levels based on colocalization analysis. In the same locus, *ZEB2* (zinc finger e-box binding homeobox 2) shows biological plausibility as a candidate gene since it plays a role as inhibitor of signal transduction in TGF- β and BMP signalling through interaction with ligand-activated SMAD proteins (Postigo et al., 2003; Conidi et al., 2011).

Colocalization analysis also supported the nomination of *EIF4EBP1* in the novel locus identified in chromosome 8. This gene encodes a translation repressor protein that competitively binds to eukaryotic translation initiation factor 4E (EIF4E) (Gingras et al., 1999; Harris and Lawrence, 2003) and is a major substrate of the mechanistic target of rapamycin (mTOR) and a key player in mTOR signalling pathway. Studies show that both *EIF4EBP1* and *EIF4E* are involved in cancer development and progression where up-regulated *EIF4E* plays an oncogenic role in carcinogenesis (Heikkinen et al., 2013; Cha et al., 2015). The same intergenic lead variant in this locus has been associated with age at menopause, and other menopause-related traits (ever had menopause and ever used HRT), supporting a plausible association with AMH levels.

We observed colocalization between our GWAS signal and variants modulating gene expression of *BMP4*. *BMP4* has a known regulatory role on AMH expression through activation of the SMAD proteins (Estienne et al., 2015; Pierre et al., 2016). Smad interacting protein 1 (also known as *ZEB2*) is one of the plausible candidate genes in chromosome 2, which would also interact with SMAD proteins and participate in AMH regulation (Postigo et al., 2003).

Our GWAS of AMH measurements revealed significant enrichment in renal system vascular morphogenesis, glomerulus vascular morphogenesis, and glomerulus morphogenesis gene set analysis. This supports the close connection between urinary and reproductive system development, originating from a common embryological origin, the intermediate mesoderm. Additionally, in our gene set enrichment results, we observed a nominally significant association with the gonadal mesoderm gene set ($P = 4.2 \times 10^{-5}$), further supporting the

interconnectedness of the urinary and reproductive systems during development. We propose that this observation may be linked to the identification of *BMP4* locus associated with AMH levels. The *BMP4* signalling pathway is crucial during kidney development, including ureteric bud outgrowth (Grinson and Rey, 2014; Nishinakamura and Sakaguchi, 2014; Oxburgh et al., 2014). This observation suggests that genetic variants affecting the renal system's development and function could influence AMH levels in women later in life. To gain further insight, studying AMH levels in younger cohorts and conducting sex-stratified analyses may be valuable in understanding the association between urogenital development and AMH levels in postnatal stages.

Tissue expression analysis also identified enrichment in the pituitary gland, although this did not reach significance after multiple testing correction. This result goes in line with research from recent years showing that AMH has versatile actions in different levels of the hypothalamus–pituitary–gonadal axis (Silva and Giacobini, 2021), further supporting the developmental alterations of neuroendocrine circuits regulating fertility.

We identified three significant genetic correlations which align with the observations in Verdiesen et al., (2022) indicating a strong positive genetic correlation between AMH and traits reflecting age at menopause, suggesting shared underlying genetic risk factors and supporting AMH as a proxy for ovarian reserve. However, it remains to be determined whether the identified genes play a direct role in regulating AMH expression or are somehow involved in folliculogenesis and thus by proxy are associated with AMH levels. While our results likely provide information about ovarian reserve/folliculogenesis genetic risk factors, future studies aiming to identify genetic risk factors underlying follicle count, early menopause, or POI may validate or expand the current findings. We also found interesting nominal significant associations, pointing towards a shared genetic background, between AMH levels and breast cancer, consistent with epidemiological studies (Ge et al., 2018). We hypothesize both *MCM8* and *CHEK2* loci may play a role in this relation and Mendelian randomization studies with independent samples could further investigate the direction of this association.

Upon querying the AMH GWAS lead variants and variants in high LD with those in other traits, we found shared significant signals among known epidemiological associations (Homburg and Crawford, 2014; De Kat et al., 2017; Ge et al., 2018; Moolhuijsen and Visser, 2020) with AMH, such as PCOS, breast cancer, postmenopausal status (age at menopause, estradiol levels, heel bone mineral density), and cardiovascular disease. Additionally, we observed novel associations with other traits in European ancestry studies, including uterine fibroids (coming from signal in *MCM8*) and blood cell counts (coming from signals near *CHEK2*), which has been also associated recently with clonal hematopoiesis (Kar et al., 2022). Further epidemiological studies assessing the potential causal relations between these traits and AMH levels are warranted to better understand the mechanisms underlying these associations.

Our study has several strengths, including the addition of a founder population, which allowed us to identify novel rare variants associated with AMH levels. Furthermore, a younger cohort and equal age of measurement from 2619 women increases the variability of AMH levels and boosts the power to detect associations. We also performed colocalization analysis for the first time, which provides a refinement for the characterization of possible regulatory effects of the genetic variants on different transcripts and genes, and to detect significant gene set enrichment. Our study has some limitations to consider. First, we only

included women of European ancestry, and our findings may not be generalizable to other populations. Second, as with other reproductive phenotypes, the lack of sufficiently sized datasets from relevant tissue in commonly used gene expression databases hinders a more reliable assessment of the mechanisms underlying regulatory effects in reproductive tissues.

In conclusion, our study expands our understanding of the genetic determinants of serum AMH levels in pre-menopausal women by identifying new loci associated with serum AMH concentration. Our results highlight the increased power of founder populations and larger sample sizes to boost the discovery of novel trait-associated variants underlying variation in AMH levels and to explore plausible genetic regulatory effects of the variants identified. Further studies are needed to validate our findings and to explore the biological mechanisms underlying the identified associations.

Supplementary data

Supplementary data are available at *Human Reproduction* online.

Data availability

The GWAS summary statistics are uploaded to the GWAS Catalogue under accession code GCST90428625.

Acknowledgements

We thank the participants and investigators of the FinnGen study and the NFBC1966 study. Part of the computations were performed in the High-Performance Computing Center of the University of Tartu.

Authors' roles

N.P.-G. conceptualized the study, N.P.-G., M.K.K., U.V., and J.R. contributed to data acquisition, N.P.-G. performed the analyses, N.P.-G. created the draft of the manuscript, T.T.P., T.L., R.K.A., and R.M. supervised the study, and all authors reviewed and approved the manuscript.

Funding

European Union's Horizon 2020 Research and Innovation Programme under the MATER Marie Skłodowska-Curie (813707) and Oulu University Scholarship Foundation and Paulon Säätiö Foundation (N.P.-G.), Academy of Finland, Sigrid Jusélius Foundation, Novo Nordisk, University of Oulu, Roche Diagnostics (T.T.P.), Estonian Research Council (1911 to R.M.). J.R. was supported by the European Union's Horizon 2020 Research and Innovation Program under Grant Agreements No. 874739 (LongITools), 824989 (EUCAN-Connect), 848158 (EarlyCause), and 733206 (LifeCycle). U.V. was supported by the Estonian Research Council (PRG, PRG1291). The NFBC1966 received financial support from University of Oulu (24000692), Oulu University Hospital (24301140), and ERDF European Regional Development Fund (539/2010 A31592).

Conflict of interest

T.T.P. has received grants from Roche, Perkin Elmer, and honoraria for scientific presentations from Gedeon Richter, Exeltis, Astellas, Roche, Stragen, Astra Zeneca, Merck, MSD, Ferring,

Duodecim, and Ajaton Terveys. There are no other conflict of interests.

References

- Ahn J, Urist M, Prives C. The Chk2 protein kinase. *DNA Repair (Amst)* 2004;**3**:1039–1047.
- Bulik-Sullivan B, Loh PR, Finucane HK, Ripke S, Yang J, Patterson N, Daly MJ, Price AL, Neale BM, Corvin A et al.; Schizophrenia Working Group of the Psychiatric Genomics Consortium. LD score regression distinguishes confounding from polygenicity in genome-wide association studies. *Nat Genet* 2015;**47**:291–295.
- Cha YL, Li PD, Yuan LJ, Zhang MY, Zhang YJ, Rao HL, Zhang HZ, Zheng XFS, Wang HY. EIF4EBP1 overexpression is associated with poor survival and disease progression in patients with hepatocellular carcinoma. *PLoS One* 2015;**10**:e0117493.
- Conidi A, Cazzola S, Beets K, Coddens K, Collart C, Cornelis F, Cox L, Joke D, Dobrev MP, Dries R et al. Few Smad proteins and many Smad-interacting proteins yield multiple functions and action modes in TGFβ/BMP signaling in vivo. *Cytokine Growth Factor Rev* 2011;**22**:287–300.
- Day FR, Ruth KS, Thompson DJ, Lunetta KL, Pervjakova N, Chasman DI, Stolk L, Finucane HK, Sulem P, Bulik-Sullivan B et al.; LifeLines Cohort Study. Large-scale genomic analyses link reproductive aging to hypothalamic signaling, breast cancer susceptibility and BRCA1-mediated DNA repair. *Nat Genet* 2015;**47**:1294–1303.
- Estienne A, Pierre A, Di Clemente N, Picard JY, Jarrier P, Mansanet C, Monniaux D, Fabre S. Anti-Müllerian hormone regulation by the bone morphogenetic proteins in the sheep ovary: deciphering a direct regulatory pathway. *Endocrinology* 2015;**156**:301–313.
- Finkelstein JS, Lee H, Karlamangla A, Nee RM, Slus PM, Burnett-Bowie SAM, Darakananda K, Donaho PK, Harlo SD, Prizan SH et al. Antimüllerian hormone and impending menopause in late reproductive age: the study of women's health across the nation. *J Clin Endocrinol Metab* 2020;**105**:E1862–E1871.
- Foley CN, Staley JR, Breen PG, Sun BB, Kirk PDW, Burgess S, Howson JMM. A fast and efficient colocalization algorithm for identifying shared genetic risk factors across multiple traits. *Nat Commun* 2021;**12**:764.
- Ge W, Clendenen TV, Afanasyeva Y, Koenig KL, Agnoli C, Brinton LA, Dorgan JF, Eliassen AH, Falk RT, Hallmans G et al. Circulating anti-Müllerian hormone and breast cancer risk: a study in ten prospective cohorts. *Int J Cancer* 2018;**142**:2215–2226.
- Gingras AC, Raught B, Sonenberg N. eIF4 initiation factors: effectors of mRNA recruitment to ribosomes and regulators of translation. *Annu Rev Biochem* 1999;**68**:913–963.
- Griffin WC, Trakselis MA. The MCM8/9 complex: a recent recruit to the roster of helicases involved in genome maintenance. *DNA Repair (Amst)* 2019;**76**:1–10.
- Grinspon RP, Rey RA. When hormone defects cannot explain it: malformative disorders of sex development. *Birth Defects Res C Embryo Today* 2014;**102**:359–373.
- Harris TE, Lawrence CJ. TOR signaling. *Sci STKE* 2003;**2003**:re15.
- Heikkinen T, Korpela T, Fagerholm R, Khan S, Aittomäki K, Heikkilä P, Blomqvist C, Carpén O, Nevanlinna H. Eukaryotic translation initiation factor 4E (eIF4E) expression is associated with breast cancer tumor phenotype and predicts survival after anthracycline chemotherapy treatment. *Breast Cancer Res Treat* 2013;**141**:79–88.
- Homburg R, Crawford G. The role of AMH in anovulation associated with PCOS: a hypothesis. *Hum Reprod* 2014;**29**:1117–1121.
- Hoyos LR, Visser JA, McLuskey A, Chazenbalk GD, Grogan TR, Dumesic DA. Loss of anti-Müllerian hormone (AMH)

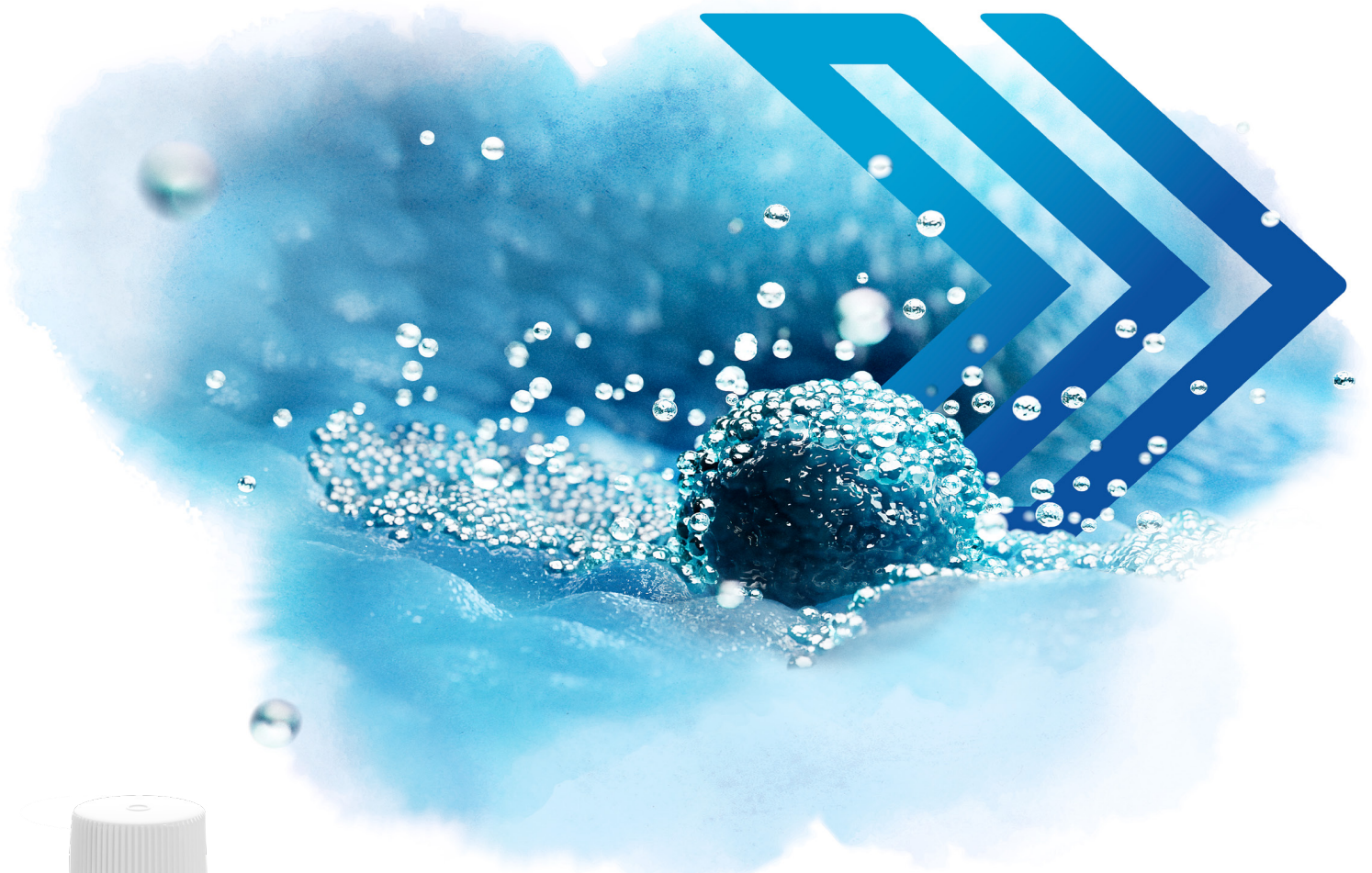
- immunoactivity due to a homozygous AMH gene variant rs10417628 in a woman with classical polycystic ovary syndrome (PCOS). *Hum Reprod* 2020;**35**:2294–2302.
- Kar SP, Quiros PM, Gu M, Jiang T, Mitchell J, Langdon R, Iyer V, Barcena C, Vijayabaskar MS, Fabre MA et al. Genome-wide analyses of 200,453 individuals yield new insights into the causes and consequences of clonal hematopoiesis. *Nat Genet* 2022;**54**:1155–1166.
- Kat AC, De Monique Verschuren W, Eijkemans MJC, Broekmans FJM, Schouw Y, Van Der. Anti-Müllerian hormone trajectories are associated with cardiovascular disease in women: results from the Doetinchem Cohort Study. *Circulation* 2017;**135**:556–565.
- Kent WJ, Sugnet CW, Furey TS, Roskin KM, Pringle TH, Zahler AM, Haussler D. The human genome browser at UCSC. *Genome Res* 2002;**12**:996–1006.
- Kentistou KA, Kaisinger LR, Stankovic S, Vaudel M, de Oliveira EM, Messina A, Walters RG, Liu X, Busch AS, Helgason H et al.; China Kadoorie Biobank Collaborative Group. Understanding the genetic complexity of puberty timing across the allele frequency spectrum. medRxiv. doi: 10.1101/2023.06.14.23291322, 2023, preprint: not peer reviewed.
- Kerimov N, Hayhurst JD, Peikova K, Manning JR, Walter P, Kolberg L, Samoviča M, Sakthivel MP, Kuzmin I, Trevanion SJ et al. A compendium of uniformly processed human gene expression and splicing quantitative trait loci. *Nat Genet* 2021;**53**:1290–1299.
- Kurki MI, Karjalainen J, Palta P, Sipilä TP, Kristiansson K, Donner KM, Reeve MP, Laivuori H, Aavikko M, Kaunisto MA et al.; FinnGen. provides genetic insights from a well-phenotyped isolated population. *Nature* 2023;**613**:508–518.
- Lutzmann M, Bernex F, da Costa de Jesus C, Hodroj D, Marty C, Plo I, Vainchenker W, Tosolini M, Forichon L, Bret C et al. MCM8- and MCM9 deficiencies cause lifelong increased hematopoietic DNA damage driving p53-dependent myeloid tumors. *Cell Rep* 2019;**28**:2851–2865.e4.
- Mägi R, Morris AP. GWAMA: software for genome-wide association meta-analysis. *BMC Bioinformatics* 2010;**11**:288.
- McCaw ZR, Lane JM, Saxena R, Redline S, Lin X. Operating characteristics of the rank-based inverse normal transformation for quantitative trait analysis in genome-wide association studies. *Biometrics* 2020;**76**:1262–1272.
- Michailidou K, Lindström S, Dennis J, Beesley J, Hui S, Kar S, Lemaçon A, Soucy P, Glubb D, Rostamianfar A et al.; ConFab/AOCS Investigators. Association analysis identifies 65 new breast cancer risk loci. *Nature* 2017;**551**:92–94.
- Moolhuijsen LME, Visser JA. Anti-Müllerian hormone and ovarian reserve: update on assessing ovarian function. *J Clin Endocrinol Metab* 2020;**105**:3361–3373.
- Nishinakamura R, Sakaguchi M. BMP signaling and its modifiers in kidney development. *Pediatr Nephrol* 2014;**29**:681–686.
- Nordström T, Miettunen J, Auvinen J, Ala-Mursula L, Keinänen-Kiukaanniemi S, Veijola J, Järvelin M-R, Sebert S, Männikkö M. Cohort profile: 46 years of follow-up of the Northern Finland Birth Cohort 1966 (NFBC1966). *Int J Epidemiol* 2022;**50**:1786–1787.
- Oxburgh L, Brown AC, Muthukrishnan SD, Fetting JL. Bone morphogenetic protein signaling in nephron progenitor cells. *Pediatr Nephrol* 2014;**29**:531–536.
- Park J, Long DT, Lee KY, Abbas T, Shibata E, Negishi M, Luo Y, Schimenti JC, Gambus A, Walter JC et al. The MCM8-MCM9 complex promotes RAD51 recruitment at DNA damage sites to facilitate homologous recombination. *Mol Cell Biol* 2013;**33**:1632–1644.
- Pierre A, Estienne A, Racine C, Picard JY, Fanchin R, Lahoz B, Alabart JL, Folch J, Jarrier P, Fabre S et al. The bone morphogenetic protein 15 up-regulates the anti-Müllerian hormone receptor expression in granulosa cells. *J Clin Endocrinol Metab* 2016;**101**:2602–2611.
- Piltonen TT, Komsu E, Morin-Papunen LC, Korhonen E, Franks S, Järvelin M-R, Arffman RK, Ollila M-M. AMH as part of the diagnostic PCOS workup in large epidemiological studies. *Eur J Endocrinol* 2023;**188**:547–554.
- Postigo AA, Depp JL, Taylor JJ, Kroll KL. Regulation of Smad signaling through a differential recruitment of coactivators and corepressors by ZEB proteins. *EMBO J* 2003;**22**:2453–2462.
- Ruth KS, Day FR, Hussain J, Martínez-Marchal A, Aiken CE, Azad A, Thompson DJ, Knoblochova L, Abe H, Tarry-Adkins JL et al; 23andMe Research Team. Genetic insights into biological mechanisms governing human ovarian ageing. *Nature* 2021;**596**:393–397.
- Ruth KS, Soares ALG, Borges MC, Eliassen AH, Hankinson SE, Jones ME, Kraft P, Nichols HB, Sandler DP, Schoemaker MJ et al. Genome-wide association study of anti-Müllerian hormone levels in pre-menopausal women of late reproductive age and relationship with genetic determinants of reproductive lifespan. *Hum Mol Genet* 2019;**28**:1392–1401.
- Schuh-Huerta SM, Johnson NA, Rosen MP, Sternfeld B, Cedars MI, Reijo Pera RA. Genetic markers of ovarian follicle number and menopause in women of multiple ethnicities. *Hum Genet* 2012;**131**:1709–1724.
- Silva MSB, Giacobini P. New insights into anti-Müllerian hormone role in the hypothalamic-pituitary-gonadal axis and neuroendocrine development. *Cell Mol Life Sci* 2021;**78**:1.
- Tyrmi JS, Arffman RK, Pujol-Gualdo N, Kurra V, Morin-Papunen L, Sliz E, Piltonen TT, Laisk T, Kettunen J, Laivuori H; FinnGen Consortium, Estonian Biobank Research Team. Leveraging Northern European population history: novel low-frequency variants for polycystic ovary syndrome. *Hum Reprod* 2022;**37**:352–365.
- Verdiesen RMG, Schouw YT, Van Der Gils CH, Van Verschuren WMM, Broekmans FJM, Borges MC, Gonçalves Soares AL, Lawlor DA, Eliassen AH, Kraft P et al. Genome-wide association study meta-analysis identifies three novel loci for circulating anti-Müllerian hormone levels in women. *Hum Reprod* 2022;**37**:1069–1082.
- Watanabe K, Taskesen E, van Bochoven A, Posthuma D. Functional mapping and annotation of genetic associations with FUMA. *Nat Commun* 2017;**8**:1826.
- Weenen C, Laven JSE, Von Bergh ARM, Cranfield M, Groome NP, Visser JA, Kramer P, Fauser BCJM, Themmen APN. Anti-Müllerian hormone expression pattern in the human ovary: potential implications for initial and cyclic follicle recruitment. *Mol Hum Reprod* 2004;**10**:77–83.

© The Author(s) 2024. Published by Oxford University Press on behalf of European Society of Human Reproduction and Embryology.
This is an Open Access article distributed under the terms of the Creative Commons Attribution-NonCommercial License (<https://creativecommons.org/licenses/by-nc/4.0/>), which permits non-commercial re-use, distribution, and reproduction in any medium, provided the original work is properly cited. For commercial re-use, please contact journals.permissions@oup.com
Human Reproduction, 2024, 39, 1564–1572
<https://doi.org/10.1093/humrep/deae117>
Original Article



Put your patients one step ahead

- SAGE 1-Step™ GM-CSF medium is the first single-step culture and transfer medium containing the GM-CSF cytokine and Hyaluronan.
- GM-CSF supports embryo-endometrial communication for improved implantation and chances of pregnancy.¹
- Provides an additional treatment option for patients with a previous failed treatment cycle.²



Upgrade your lab with
innovation that matters.

[Click to explore](#)



CooperSurgical®

1. Hardy, K. & Spanos, S. (2002) Growth factor expression and function in the human and mouse preimplantation embryo. J Endocrinol 172: 221-236.
2. Sipahi, M., Mümüşoğlu, S. et al. (2021). The impact of using culture media containing granulocyte-macrophage colony-stimulating factor on live birth rates in patients with a history of embryonic developmental arrest in previous in vitro fertilization cycles. Journal of the Turkish German Gynecological Association, 22(3), 181-186.